

PLATINUM-GROUP MINERAL ASSEMBLAGES AND CHROMITE COMPOSITION IN THE ALTERED AND DEFORMED BACURI COMPLEX, AMAPA, NORTHEASTERN BRAZIL

HAZEL M. PRICHARD[§]

Department of Earth Sciences, University of Cardiff, P.O. Box 914, CF10 3YE, Wales, U.K.

J. HAROLDO S. SÁ[§]

Departamento de Geologia, Universidade Federal da Bahia, 40.170-290 Salvador, Bahia, Brazil

PETER C. FISHER

Department of Earth Sciences, University of Cardiff, P.O. Box 914, CF10 3YE, Wales, U.K.

ABSTRACT

In the Bacuri complex, Amapa, Brazil, there is good evidence for Pd mobility both during serpentinization and lateritization. In non-lateritized, serpentinized samples, Pd bismuthide occurs with chalcopyrite in chlorite-filled veins that cross-cut serpentine and chromite probably only a few tens of micrometers from the source of the platinum-group elements (PGE). Low Pt/Pd values of less than one are characteristic of magmatic values, and sporadic higher values of up to 4 indicate partial removal of Pd. The highest Pt/Pd values (up to 26) occur in laterites, where Pt remains but Pd has been extensively removed. The PGE are concentrated in non-lateritized rock-types including chromitite, serpentinite containing disseminated chromite, and sulfide-bearing serpentinite. The highest whole-rock PGE concentrations are 166 ppb Pt and 609 ppb Pd. Osmium, Ir and Ru concentrations in the chromitite can be attributed to the presence of laurite and irarsite, whereas sulfide-bearing serpentinite contains sperrylite. Pd-Bi tellurides, including sobolevskite and michenerite, are the most common platinum-group minerals. They commonly occur with pentlandite and (less common) pyrrhotite, typically partially altered to millerite, magnetite, pyrite, nickeloan pyrrhotite, maucherite and gersdorffite, all of which form less than 1% of these rocks. Chromitite in folded layers 3–4 m thick has Cr/(Cr + Al) values of 69.0–84.1, Mg/(Mg + Fe²⁺) values of 27.6–51.4, and TiO₂ values of up to 1.69%, compositions most typical of chromite from a stratiform complex of continental origin.

Keywords: platinum-group elements, platinum-group minerals, Amazon, chromite, lateritization, serpentinization, Bacuri complex, Amapa, Brazil.

SOMMAIRE

Le complexe igné de Bacuri, dans l'état d'Amapa, au Brésil, présente de l'évidence probante en faveur de la mobilisation du palladium au cours de la serpentinisation aussi bien que de la latéritisation. Dans les échantillons serpentinisés non latéritisés, on trouve un bismuthure de Pd avec la chalcopyrite dans des veines remplies de chlorite recoupant la serpentine et la chromite situées à peine quelques dizaines de micromètres de la source des éléments du groupe du platine. De faibles valeurs de Pt/Pd, inférieures à l'unité, caractérisent les roches magmatiques, tandis que des valeurs sporadiques plus élevées, jusqu'à 4, témoignent d'un lessivage partiel du Pd. Les valeurs les plus élevées de Pt/Pd (jusqu'à 26) se trouvent dans les latérites, le Pt y étant résiduel et le Pd, largement lessivé. Les éléments du groupe du platine sont concentrés dans les chromitites non latéritisées, les serpentinites contenant la chromite disséminée, et celles qui contiennent des sulfures. Les teneurs les plus élevées en éléments du groupe du platine seraient de 166 ppb Pt et 609 ppb Pd. Les teneurs d'osmium, d'iridium et de ruthénium dans les chromitites seraient dues à la présence de laurite et d'irarsite, tandis que les serpentinites sulfurées contiennent la sperrylite. Les tellurures de Pd-Bi, y inclus la sobolevskite et la michenerite, constituent les minéraux du groupe du platine les plus répandus. On les voit couramment associés à la pentlandite et, plus rarement, à la pyrrhotite, typiquement partiellement altérée à millerite, magnétite, pyrite, pyrrhotite nickelifère, maucherite et gersdorffite, le tout formant moins de 1% de ces roches. La chromitite se présente en couches de 3 à 4 m qui ont été plissées; les valeurs de Cr/(Cr + Al) vont de 69.0 à 84.1, le rapport Mg/(Mg + Fe²⁺), de 27.6 à 51.4, et les concentrations de TiO₂ atteignent 1.69%. Ces compositions sont typiques de la chromite des complexes stratiformes d'origine continentale.

(Traduit par la Rédaction)

Mots-clés: éléments du groupe du platine, minéraux du groupe du platine, Amazone, chromite, latéritisation, serpentinisation, complexe de Bacuri, Amapa, Brésil.

[§] E-mail addresses: prichard@cardiff.ac.uk, sa@ufba.br

INTRODUCTION

The Bacuri layered mafic and ultramafic complex is situated in Amapa State in the Amazon region of Brazil. It is located about 50 km south of the railroad that links the Serra do Novio manganese mining district with the port of Santana, at the mouth of the Amazon River (Fig. 1). In the 1980s, the Companhia Ferro Ligas do Amapa, a subsidiary of the Grupo CAEMI Mineração e Metalurgia S.A., discovered economic deposits of chromitite in the complex. The search for individual layers of chromitite was aided by the presence of rare remnant blocks of chromitite at the surface, soil geochemical anomalies for Cr, and drilling. A total of 70 km of drill core indicated reserves of more than 7 million tonnes of chromitite. Other occurrences of chromian spinel in the surrounding area are being studied and evaluated. Production of chromian spinel started in 1988 and stopped in 1996. During this time, exploitation removed 100,000 tonnes of ore per year and created the exposure of spectacular layers of folded chromitite 3–4 meters thick in quarry walls (Fig. 2a). In

1996, the operation was sold to ELKEM ASA, a Norwegian company, and production commenced again in 1997 with production of approximately 200,000 tonnes per year.

The Bacuri complex has received little attention in the past. Our initial aim was to determine the type of mafic and ultramafic complex represented on the basis of characteristics and geochemistry of the chromite, and to establish the nature and distribution of platinum-group elements (PGE) as a function of the type of igneous complex hosting them. PGE mineralization in chromitites in layered complexes tends to be laterally extensive at certain horizons, whereas in ophiolite complexes, the PGE are only concentrated locally. A second aim was to understand the distribution of PGE among different igneous lithologies and the effects on these concentrations of serpentinization and lateritization. Samples were taken only from drill core and included chromitites, serpentinites that host chromitites, disseminated chromite and overlying chromitite-rich laterites. In this paper, we establish the presence of PGE in the Bacuri complex and identify the

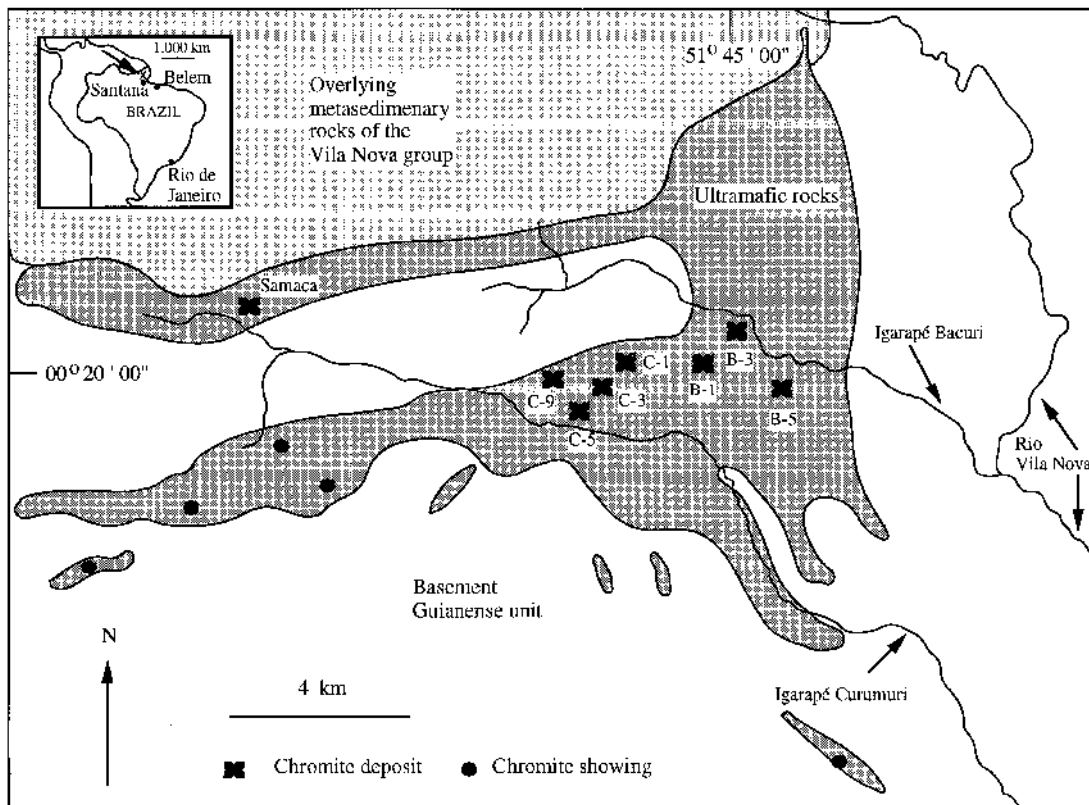
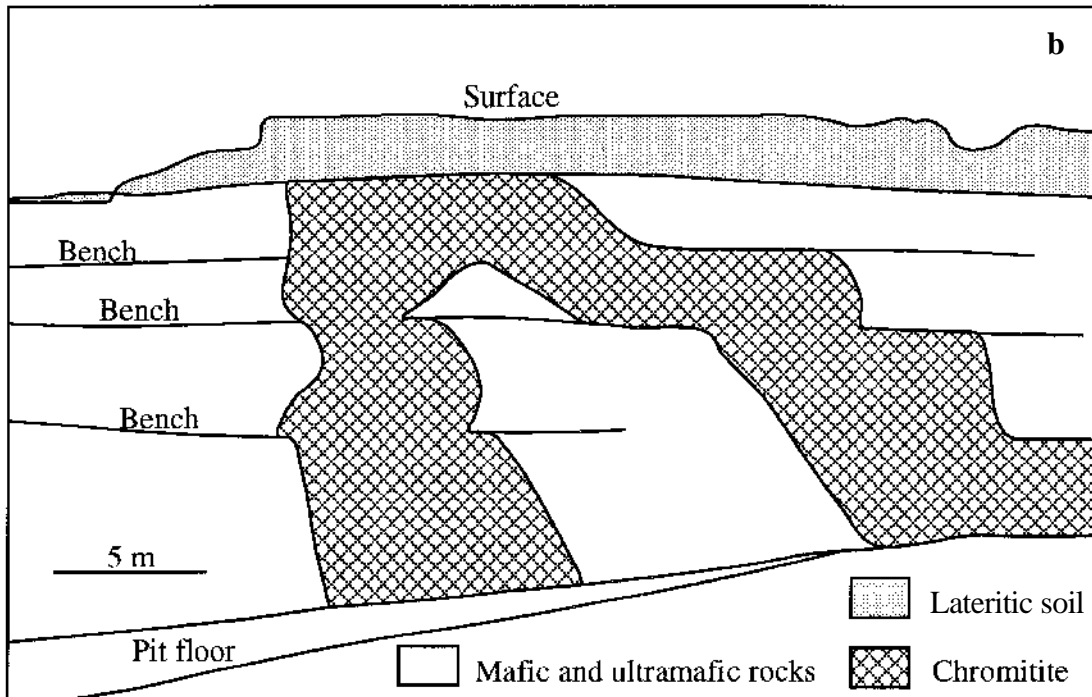


Fig. 1. Map showing the location and geology of the Bacuri complex.



a



b

FIG. 2. a. Photograph of a layer of chromitite (dark brown to black) displayed on a quarry wall and folded into an antiform, surrounded by a mixture of white altered amphibolite – gabbro and ultramafic rocks. Note the lateritic soil (“limonite”) at the top of the quarry wall and the deeply weathered (saprolitic) material underneath. Figure 2b is a sketch of Figure 2a.

mineralogical associations of the platinum-group minerals (PGM) in the serpentinized but non-lateritized igneous lithologies. These results made it possible to examine and evaluate the initial stages of Pd mobilization from its primary magmatic distribution through the stages of serpentinization and lateritization.

GENERAL GEOLOGY

The Bacuri complex intrudes the basement rocks of the Guianense Unit composed of metamorphosed plutonic and volcano-sedimentary rocks now represented by migmatites and gneisses, with a Rb/Sr age of around 2940 Ma (Montalvão & Tassinari 1984). The hanging wall to the Bacuri complex contains rocks of the Vila Nova Group, which has a basal metaconglomerate containing mafic, ultramafic and chromitite pebbles, likely derived from the Bacuri complex, overlain by schist, quartzite, metachert and iron formation giving K/Ar ages of between 1760 and 1920 Ma (Montalvão & Tassinari 1984). Thus the Bacuri complex was emplaced after deposition of the Guianense unit and prior to the Vila Nova Group, at some time during the late Archean or the early Proterozoic. Granite bodies, pegmatites, quartz veins and diabase dykes are common in the region and cross-cut all the other rock types.

The Bacuri complex occupies an area of at least 55 km², but its limits are not mapped with precision owing to the paucity of outcrops and the lateritic cover. It is composed of a sequence of rocks ranging from dunite at the base to gabbro at the top, and includes peridotite, pyroxenite, chromitite, gabbro and mafic anorthosite, now all extremely altered (Matos *et al.* 1992). The rocks are layered, and locally display cyclic units, but the orientation of the layering is quite variable, locally subvertical, and commonly disrupted, as the complex has been intensely faulted and folded (Figs. 2, 3). The scale of the folding can be observed in the quarry walls, where igneous layers are tightly folded, and one antiform, defined by a folded layer of chromitite, extends 100 m horizontally and 70 m vertically (Fig. 2a). The complex has undergone extensive serpentinization, which has changed the primary assemblage of minerals. The silicate rock types recovered in drill core are predominantly serpentinite and tremolite-talc schist.

Except in quarry walls, the rocks are very poorly exposed, covered by laterite and tropical jungle. The surface extent of the complex and the relationships among rock types are unclear, making it impossible to reconstruct the magmatic stratigraphy and the thickness of the complex. Further detailed work on drill-core material may provide some clarification of these features, but this is beyond the scope of this paper.

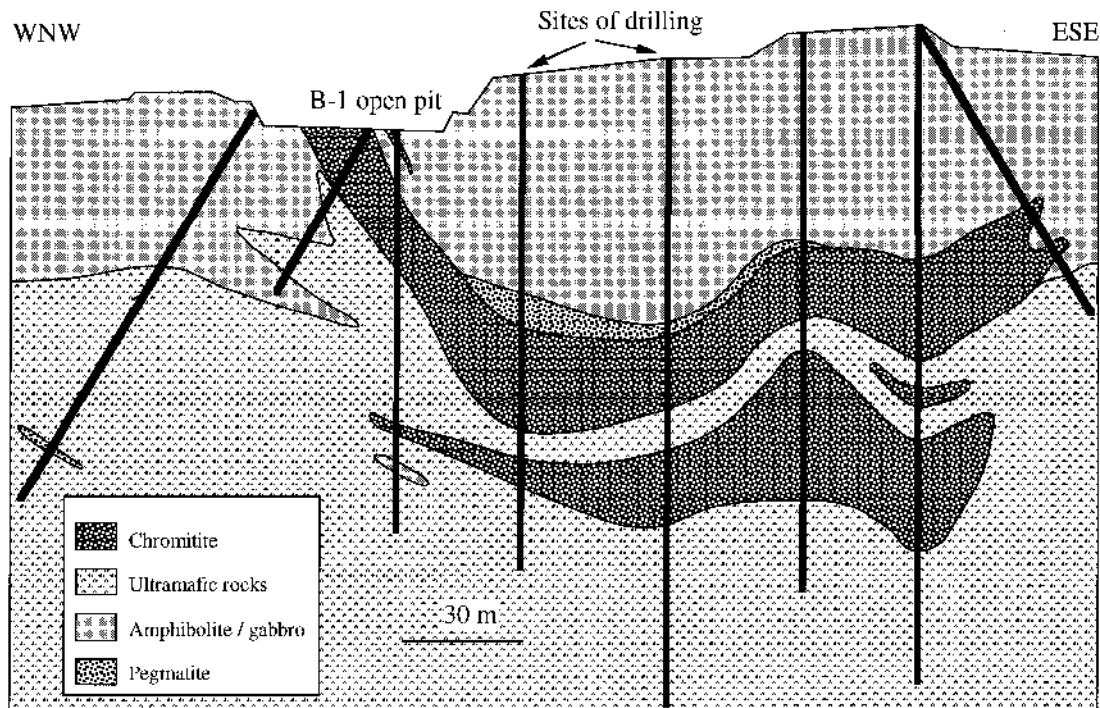


FIG. 3. Cross section of open pit (B1) showing the folded and disrupted units of chromitite reconstructed from borehole data.

CHROMITE MINERALIZATION

The chromitite layers are hosted by metaperidotite (serpentinite). Their thicknesses vary from a few centimeters to several meters, and the thickest layers of chromitite are located both at the contact between metaperidotite and metagabbro and within ultramafic units. These layers have sharp contacts with their host rocks, but disseminated chromian spinel commonly occurs within the serpentinite close to them. The chromitite is usually massive, and the grains are between 0.6 and 0.8 mm in diameter with euhedral to subhedral shapes (Fig. 4). The grains of chromian spinel commonly exhibit inclusions of serpentine and of sulfide. Locally, the chromitite shows a fragmental or "pull-apart" texture, where the grains are broken and veined. A ferrian chromite rim to the chromian spinel grains is not commonly encountered in non-lateritized samples.

COMPOSITION OF THE CHROMIAN SPINEL

Grains of chromian spinel from the non-lateritized chromitites are unzoned, with consistent major-element contents across each grain and with no distinction between the rim or center. The composition of the chromite varies much more between grains from one locality than between localities (Table 1). The range in Cr is relatively small (47.01–57.46 wt% Cr₂O₃). The value 100Cr/(Cr + Al) ranges from 69.0 to 84.1, and 100Mg/(Mg + Fe²⁺), from 27.6 to 51. This range of values justifies the term chromite for most of the suite. Fe₂O₃ shows a large range, from 0.12 to 16.01 wt%.

Minor elements such as Ti, Ni and Zn display some variation. For example, in one grain Ti content varies from 0.07 to 1.45 wt% TiO₂, which is almost equal to the entire range (0.06–1.69%) of values in the suite.

TABLE 1. TYPICAL COMPOSITIONS OF CHROMITE GRAINS, BACURI COMPLEX, NORTHEASTERN BRAZIL

	PT-20	PT-20	PT-54	PT-54	BC-12	BC-50	PT-4	PT-5
TiO ₂ wt%	0.06	0.49	0.07	1.45	0.90	0.10	0.62	0.50
Al ₂ O ₃	15.34	9.30	13.50	13.47	5.96	15.01	9.69	9.89
Cr ₂ O ₃	53.53	52.55	57.46	58.11	47.01	55.19	52.95	53.52
Fe ₂ O ₃	1.02	7.68	0.42	0.39	16.01	0.87	7.38	6.76
FeO	21.50	23.07	18.81	18.65	23.91	17.93	21.01	20.53
MnO	0.34	0.40	0.22	0.35	0.45	0.35	0.38	0.42
MgO	8.15	6.29	9.95	9.87	5.22	10.48	7.67	8.05
ZnO	0.08	0.29	0.12	0.17	0.18	0.11	0.26	0.11
NiO	0.14	0.10	0.00	0.06	0.18	0.04	0.19	0.13
total	100.16	100.17	100.56	100.54	99.82	100.10	100.14	100.01
Ti <i>apfu</i>	0.001	0.012	0.002	0.035	0.024	0.002	0.016	0.015
Al	0.591	0.373	0.516	0.513	0.246	0.570	0.384	0.391
Cr	1.383	1.415	1.472	1.434	1.302	1.406	1.409	1.420
Fe ³⁺	0.025	0.197	0.010	0.010	0.422	0.021	0.187	0.171
Fe ²⁺	0.587	0.657	0.510	0.504	0.701	0.483	0.591	0.576
Mn	0.009	0.012	0.006	0.010	0.013	0.010	0.011	0.012
Mg	0.397	0.320	0.481	0.476	0.273	0.504	0.385	0.403
Zn	0.002	0.007	0.005	0.004	0.005	0.003	0.006	0.003
Ni	0.004	0.003	0.000	0.001	0.005	0.000	0.005	0.003
total	2.990	2.995	2.999	2.987	2.991	2.999	2.994	2.994

Provenience of samples: PT-20 from quarry B-1, PT-54 from Samaca, BC-12 and BC-50 from quarry C-5, and PT-4 and PT-5, both from quarry B-5 (Fig. 1). Oxides in wt% and elements in atoms per formula unit (*apfu*). The proportions of Fe²⁺ and Fe³⁺ were calculated on the basis of charge balance.

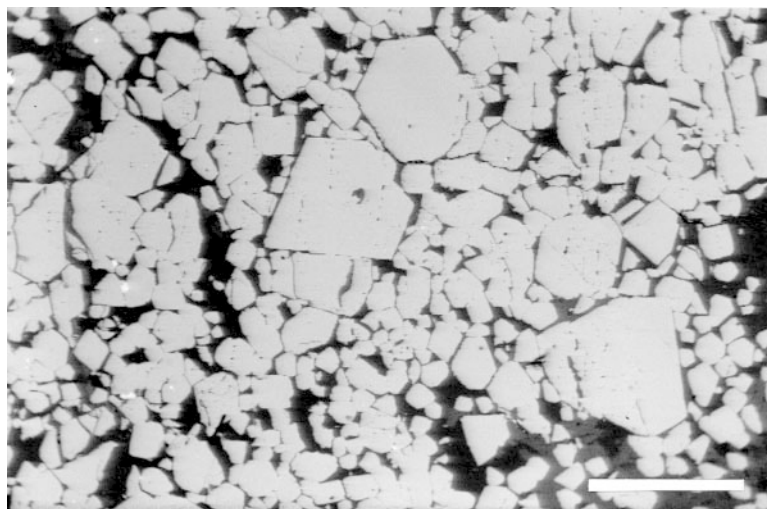


FIG. 4. Back-scattered scanning electron microscope image of typical chromitite, PT 5 from drill core CG-41, quarry B-5, showing euhedral grains of chromite with interstitial altered silicates. Scale bar represents 1 mm.

The thirty-meter chromitite unit in drill core GS295 is almost certainly an apparent thickness across the layer, but does not appear to be disrupted by folding or faulting. The forty analyses of chromite taken in a traverse through this chromitite do not reveal systematic variation in major-element proportions (Fig. 5), with ranges of 3.28–10.85% MgO, 15.90–30.34% FeO, 52.19–62.40% Cr₂O₃ and 7.32–17.32% Al₂O₃. Analysis of the spinel phase in the laterite indicates extensive, though incomplete, alteration of the chromite to ferrian chromite.

Platinum-group elements in non-lateritized rocks

The highest PGE concentrations tend to occur in the chromitite, with values of 166 ppb Pt and 570 ppb Pd, and in the serpentinite, with concentrations of 117 ppb Pt and 609 ppb Pd (Table 2). The rock type with the most samples containing 10 ppb Pt or more is serpentinite with disseminated chromite, but the maximum concentrations are not as high as in the chromitite. The PGE are generally not concentrated in the gabbro, but one gabbro sample contains 43 ppb Pt and 6 ppb Pd.

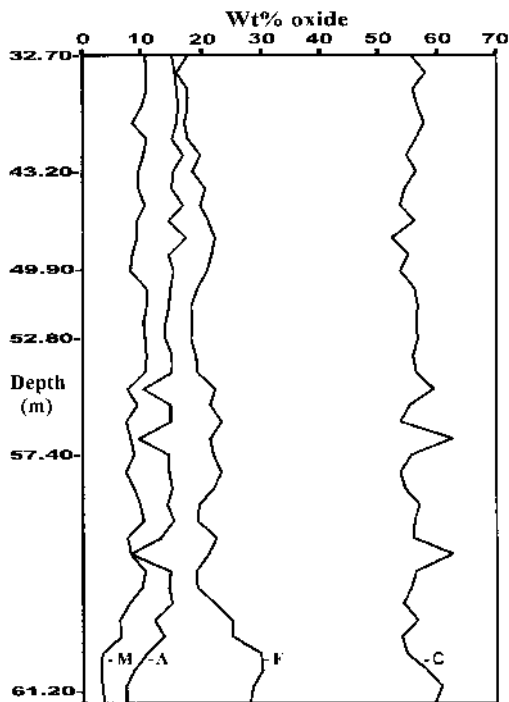


FIG. 5. Variation of MgO (M), FeO (F), Al₂O₃ (A) and Cr₂O₃ (C) in weight percent oxide in chromite with depth through a chromitite layer in bore hole GS295. Sample depths, given in meters below the surface, indicate the location of samples analyzed for all six PGE (Table 3), with the sample containing the maximum PGE located at 52.8 meters.

In the chromitite, serpentinite with disseminated chromite, and sulfur-bearing serpentinite, Pt tends to increase as Pd increases (Fig. 6). For each rock type, there are one or two high Pt and Pd values in the hundreds of ppb range, but most only have concentrations of tens of ppb, consistent with a log-normal distribution. This pattern also is observed in the results for the six chromitites taken from the sequence across the 30 m thickness of chromitite in GS295 (Table 3, Fig. 5). Of the six samples analyzed, only one sample, at 52.8 meters, 20 meters from the top of the layer, has Pt and Pd in the hundreds of ppb range (Table 4). The Pt :Pd ratio varies in the different rock-types. The average Pt: Pd value in the chromitite is 1.0, in serpentinite it is 0.6, and in serpentinite with disseminated chromite, it is 1.6 (Table 2). The one gabbro sample with greater than 10 ppb Pt has the largest Pt: Pd ratio, 7.2.

Only ten samples were analyzed for all six PGE (Table 3); eight consist of massive chromitite, one is a serpentinite with disseminated chromite, and another is a sulfide-bearing serpentinite. In the two chromitites in which Pt and Pd are most enriched, Rh, Ru, Os and Ir also are the most enriched. Ruthenium values are high in all the chromitite samples analyzed, ranging from 118 to 235 ppb, whereas the Pt and Pd values vary over a greater range, from 6 to 155 ppb and from 2 to 350 ppb, respectively. Rhodium values are low, ranging from 13 to 38 ppb. In contrast, the sulfide-bearing serpentinite has elevated Pt and Pd values, 185 and 375 ppb, respectively, but low Rh, Ru, Os and Ir values. Chondrite-normalized PGE signatures for the samples from Amapa are characteristic of their host rock-type (Fig. 7). The serpentinite pattern has a positive slope, with enrichment

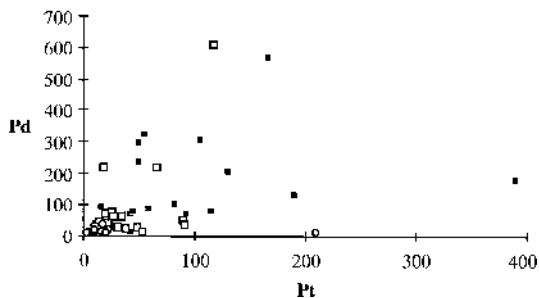


FIG. 6. Graph of Pt with Pd in a) non-lateritized chromitites and serpentinites with disseminated chromite (black squares), b) non-lateritized sulfide-bearing serpentinites (open squares) [a) and b) using data from Geosol – Minas Gerais (Table 2)], c) saprolitic samples of chromitite (also black squares) from GS295 and GS209, and d) limonitic samples from GS208 and GS209 (open circles) using data from Genalysis (Table 4). Note that the samples of “limonite” have low Pt and Pd values except for the one sample with a high Pt (210 ppb) and low Pd (8 ppb).

TABLE 2. CONCENTRATIONS OF Pt, Pd, Ni, Cu, S AND AS IN SAMPLES WITH >10 ppb Pt IN NON-LATERITIZED SAMPLES, BACURI COMPLEX, NORTHEASTERN BRAZIL

Sample	Core	Depth	Quarry	Pt	Pd	Ni	Cu	S	As	Pt/Pd
Chromitites										
BC-26	GS-209	128.5	C-5	12	16	834	7	25	5	0.75
BC-62	GS-149	61.0	B-1	16	90	911	9	50	6	0.18
BC-63	"	64.6	"	50	296	1086	11	62	5	0.17
BC-65	"	72.9	"	54	324	956	12	766	26	0.17
PT-04	CG-41	116.5	B-5	40	69	1317	7	85	4	0.58
PT-05	"	118.8	"	166	570	1915	15	813	20	0.29
PT-18	GS-156	78.5	B-1	105	304	1416	10	478	4	0.35
PT-40	GS-206	37.4	C-5	114	76	1560	24	174	14	1.5
PT-41	"	60.0	"	50	234	2615	9	25	5	0.21
Serpentinite with disseminated chromite										
BC-03	GS-209	54.8	C-5	48	25	1173	8	422	11	1.92
BC-05	"	57.8	"	38	20	1719	14	594	8	1.9
BC-12	"	76.3	"	66	218	3253	158	2490	9	0.3
BC-16	"	88.3	"	90	47	1034	17	257	7	1.91
BC-18	"	94.2	"	34	58	1034	19	305	8	0.59
BC-19	"	98.9	"	10	18	1631	18	666	6	0.56
BC-24	"	122.4	"	91	35	2316	17	2921	11	2.6
BC-31	"	148.8	"	53	12	1687	7	721	6	4.42
BC-32	"	164.7	"	31	23	1881	7	696	6	1.35
PT-09	CG-41	80.4	B-5	18	219	1590	3	25	1	0.01
Serpentinite										
BC-04	GS-209	56.8	C-5	26	75	2772	24	537	6	0.35
BC-06	"	60.7	"	20	68	3633	119	1269	9	0.29
BC-14	"	82.1	"	15	41	2902	41	1078	5	0.37
BC-20	"	103.3	"	22	36	2484	124	1489	9	0.61
BC-35	"	175.7	"	18	9	2453	27	492	12	2.0
BC-97	CG-35	48.55	B-5	27	61	4659	324	642	12	0.44
BC-104	"	86.7	"	117	609	2286	92	1332	3	0.19
BC-108	"	100.6	"	11	24	1189	186	1718	2	0.46
Gabbro										
BC-57	GS-209	243.9	C-5	43	6	79	42	427	5	7.17

Concentrations of Pt and Pd in ppb, and of Ni, Cu, S and As in ppm. Total number of samples analyzed: chromitites 70, serpentinites with disseminated chromite 15, serpentinite 35, pyroxenite 5 and gabbro 10. Depth in meters. Quarry locations B-1, B-5 and C-5, are given in Figure 1.

TABLE 3. CONCENTRATIONS OF SIX PGE IN SAMPLES FROM THE THICK CHROMITITE LAYER IN GS295 AND SAMPLES WITH HIGH Pt AND Pd VALUES IN TABLE 2, BACURI COMPLEX, NORTHEASTERN BRAZIL

Sample	Pt	Pd	Ru	Rh	Os	Ir
GS295, 32.7 m	42	10	186	13	74	76
GS295, 43.2 m	8	18	126	14	28	32
GS295, 49.9 m	10	18	205	17	44	42
GS295, 52.8 m	130	205	235	38	88	98
GS295, 57.4 m	10	15	175	14	88	84
GS295, 61.2 m	6	2	165	17	54	52
PT-05a	155	359	205	22	172	138
PT-18a	100	195	118	24	76	60
BC-12a	40	147	195	15	88	42
BC-104a	185	375	40	27	10	12

Results in ppb. Eight samples of chromitite, along with serpentinite with disseminated chromite (BC-12a) and a sulfide-bearing serpentinite (BC-104a).

in Pt and Pd, whereas the chromite-rich samples have flatter patterns, with a positive Ru anomaly and a Pd anomaly varying from positive to negative.

There are no consistent correlations of Pt and Pd with Cu or Ni concentrations. Some samples with enriched Pt and Pd have higher values of Cu, Ni, S and As than those with undetected Pt and Pd. Among the six sets of analytical data from GS295, the sample with the highest PGE values, by an order of magnitude, also has the highest Ni value, possibly indicating saturation of the magma in a sulfide liquid at this level within the chromitite layer. There is nothing unusual about the geochemistry of this PGE-rich chromitite compared with that of the rest of the layer (Fig. 5). There is a relationship, however, between the low Pt:Pd ratio occur-

TABLE 4. CONCENTRATIONS OF Pt, Pd AND TRACE ELEMENTS IN SAMPLES OF LIMONITIC LATERITE AND SAPPROLITE, BACURI COMPLEX, NORTHEASTERN BRAZIL

Sample	Pt	Pd	V	Co	As	Zr	Rb	Pb	Sn	Zn	Cu	Ni
GS208, 0.7 m	17	23	665	nd	95	52	7	15	5	61	nd	106
GS208, 0.8 m	17	5	665	3	41	13	8	1	13	261	nd	165
GS208, 1.4 m	22	18	724	nd	82	28	9	5	3	75	nd	107
GS208, 2.3 m	15	12	706	nd	91	23	6	1	3	44	nd	107
GS208, 3.3 m	23	15	731	nd	98	28	9	nd	7	44	nd	206
GS208, 4.1 mS	15	19	434	nd	125	25	6	nd	4	53	nd	74
GS208, 4.8 mS	9	17	304	nd	114	22	8	6	6	38	nd	56
GS208, 5.2 m	10	15	389	nd	134	25	11	3	nd	50	nd	88
GS208, 5.5 m	6	9	414	nd	76	87	10	2	6	78	nd	44
GS208, 5.8 m	6	10	283	nd	46	35	8	nd	6	80	nd	38
GS208, 6.8 m	12	7	588	nd	77	23	9	nd	5	155	nd	96
GS208, 7.2 m	14	10	490	nd	52	22	6	nd	2	148	nd	103
GS208, 7.5 m	10	7	529	1	64	20	5	1	6	161	nd	129
GS208, 8.5 m	210	8	975	nd	43	124	10	nd	7	420	4	134
GS209, 4.1 mS	5	6	362	nd	37	972	7	6	13	42	nd	36
GS209, 5.7 mS	9	12	628	nd	89	35	11	nd	4	40	nd	33
GS209, 6.5 m	7	13	720	nd	100	38	8	2	4	41	nd	37
GS209, 6.7 mS	8	9	352	nd	64	52	9	4	5	43	nd	28
GS209, 6.9 mS	3	4	712	nd	132	71	8	nd	5	43	nd	30
GS209, 7.6 m	8	11	666	nd	76	75	8	nd	3	64	nd	105
GS209, 7.9 m	11	10	783	19	37	19	9	nd	5	207	nd	201
GS209, 8.5 mS	4	12	256	nd	32	526	11	5	13	38	nd	44
GS209, 39.6 m	58	84	558	42	36	15	8	5	12	124	26	447
GS209, 40.6 mS	82	100	492	nd	47	20	9	nd	11	65	58	753
GS209, 41.6 m	92	68	1339	28	23	6	9	6	4	141	nd	494
GS209, 42.6 m	390	180	1214	14	41	10	9	2	1	94	17	670
GS209, 43.6 mS	190	130	329	47	44	29	10	nd	4	50	34	790
GS209, 44.6 mS	42	70	332	40	46	13	10	nd	13	44	33	662
GS209, 45.6 mS	44	78	305	61	46	11	7	2	14	52	65	886
GS209, 47.4 mS	20	34	159	117	17	10	8	2	7	88	18	738
GS209, 48.3 mS	21	56	102	238	40	12	6	2	11	57	35	1438
GS209, 49.0 mS	11	36	35	138	11	15	8	4	6	34	38	996
GS209, 50.2 mS	18	40	80	140	21	10	10	3	7	49	28	1055
GS209, 51.1 m	17	12	834	152	nd	7	7	nd	5	233	nd	695
GS295, 32.7 m	42	10	468	85	2	9	10	nd	1	130	nd	478
GS295, 43.2 m	8	18	430	85	11	7	31	nd	2	87	nd	809
GS295, 49.9 m	10	18	406	78	6	10	27	nd	nd	484	nd	824
GS295, 52.8 m	130	205	368	87	9	10	24	nd	1	115	nd	930
GS295, 57.4 m	10	16	378	85	9	9	72	1	2	497	nd	714
GS295, 61.2 m	6	2	291	73	0	10	24	nd	1	254	nd	851

Concentrations of Pt and Pd are expressed in ppb, those of other trace elements, in ppm, except for Cr, in %. S: Serpentinites with some disseminated chromite. All the other samples consist of chromitite. Samples of "limonite": GS208 and GS209 4.1-8.5 m. Samples of saprolite: GS209 39.6-51.1 m and GS295. Sample GS295 is from quarry C1, whereas samples GS208 and GS209 are from quarry C5 (Fig. 1). nd represents non-detected.

ring with high Cu values both in the serpentinite with disseminated chromite and in the sulfur-bearing serpentinite samples. This correlation occurs irrespective of whether the samples have high or low Pd values (Fig. 8).

PLATINUM-GROUP ELEMENTS IN LATERITES

The laterites on the Bacuri complex can be divided into a brown limonitic zone that may be as much as 10 meters thick and an underlying saprolitic zone tens of meters thick in which the different parent mafic and ultramafic lithologies may be distinguished and the tectonic folding and faulting can still be recognized. This saprolitic zone is very colorful, as it intersects altered white gabbro, altered yellow ultramafic samples, and orange, red and black altered chromite-bearing samples. These two lateritic units can be seen clearly in the quarry walls (Fig. 2).

Two adjacent drill-cores (GS208 and GS209) containing 8.5-m sections of the limonitic zone were chosen for analysis. Remnants of massive and disseminated chromite can be observed in this limonitic zone. Of the 22 samples of "limonite" sampled, 14 were classed as originally chromitites (Table 4). Platinum and Pd values range from 3 to 23 ppb and 4 to 23 ppb, respectively, in all the "limonite" samples, except for one chromitite. This is the lowest sample collected, 8.5 m below the surface in GS208, and has a Pt concentration of 210 ppb, a Pd concentration of 8 ppb (Fig. 6) and a resultant very high Pt:Pd ratio of 26. This sample of chromitite with enriched Pt presumably reflects the distribution of Pt in the non-lateritized samples, where Pt values of one hundred ppb or more are sporadic. The

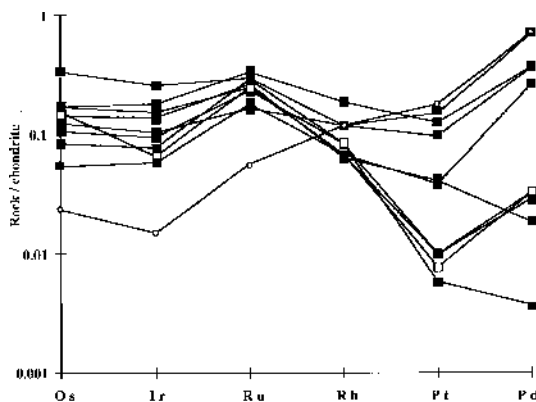


FIG. 7. Chondrite-normalized PGE patterns for eight samples of chromitite (black squares), a sulfide-bearing serpentinite (open circles) and a chromite-rich serpentinite (open squares). Values for chondrite (in ppb) are: Os 514, Ir 540, Ru 690, Rh 200, Pt 1025, and Pd 545, taken from Naldrett & Duke (1980).

low Pd value associated with this high Pt value is not typical of the non-lateritized samples, however, suggesting that the original sample had high Pt and Pd concentrations, and that the Pd has been removed.

The trace elements in the limonitic samples show a depletion in Co, Ni and Cu compared to underlying chromitite (Table 4, Fig. 9) and an increase in As and Zr contents. The limonitic samples, however, are so altered that the percentage of chromite in their protolith lithology is uncertain. The proportion of these trace elements thus may not be a true representation of those resulting from lateritization of massive chromitite.

Twelve samples from GS209 taken between depths of 39.6 and 51.1 m have the visual appearance of saprolitic laterites, with white, orange and brown coloration, but their geochemistry is more characteristic of non-lateritized lithologies, with much less depletion in Pt, Pd, Ni and Cu. Six samples of chromitite from GS295 taken from between 32 and 61 meters, classified here as saprolitic, show generally lower concentrations of Pt, Pd, Ni and Cu than samples of chromitite from deeper positions (compare non-lateritized samples of chromitite in Table 2 with saprolitic samples of chromitite in Table 4).

SULFIDE MINERALOGY

Sulfides in non-lateritized rocks are not abundant, forming much less than 1% of the mode. However,

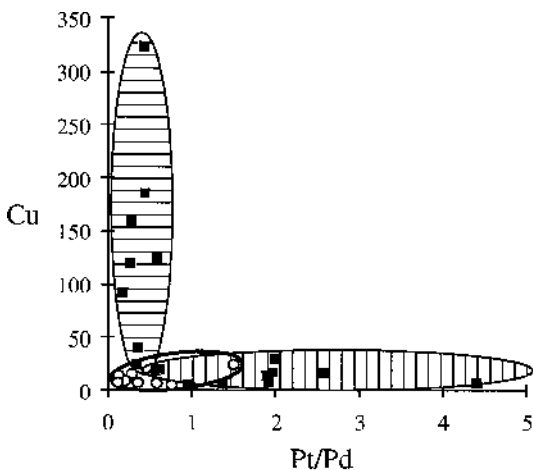


FIG. 8. Graph of Cu versus Pt/Pd for non-lateritized samples of chromitite (open circles: group outlined in bold) and for samples of non-lateritized serpentinite with disseminated chromite or sulfides (black squares). This latter group can be divided into samples with a low Pt:Pd ratio and moderate to high Cu, indicating Pd reconcentration (horizontal hatching), and samples with a moderate to high Pt:Pd ratio and low Cu (vertical line hatching).

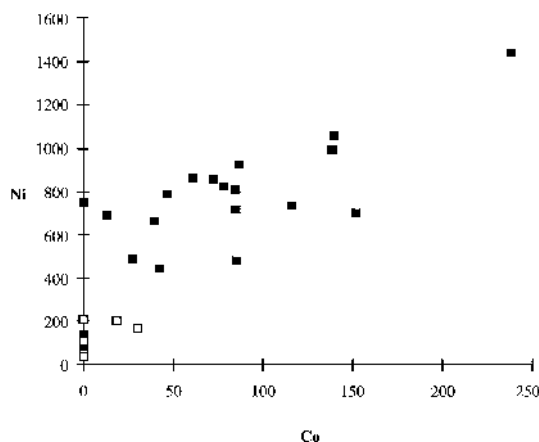


FIG. 9. Graph of Ni versus Co concentration for saprolite samples of ultramafic rock (black squares), both from GS295 and GS209, and limonitic samples (open squares) from GS208 and GS209 (Table 4).

TABLE 5. TYPICAL COMPOSITIONS OF SULFIDES AND ARSENIDES, BACURI COMPLEX, NORTHEASTERN BRAZIL

	1	2	3	4	5	6	7
Fe wt%	28.43	24.30	0.88	41.58	2.81	3.50	0.94
Ni	37.39	41.88	63.95	4.19	46.74	22.65	34.94
Co	1.06	0.55		0.91		10.73	0.78
S	32.82	33.63	35.07	52.39		18.36	18.67
As					43.17	45.21	40.59
Se							1.97
total	99.71	100.36	99.89	99.06	92.73	100.45	99.78

Samples: 1 pentlandite in BC104 (Table 2), 2 pentlandite in PT18 (Table 2), 3 millerite in BC65 (Table 2), 4 pyrite in PT18, 5 maucherite in BC104, 6 gersdorffite in PT18, and 7 selenian gersdorffite in BC65.

- $(\text{Ni}_{1.0}\text{Fe}_{0.9}\text{Co}_{0.14})_{28.8}\text{S}_8$

PGM are typically associated with them and, therefore, their parageneses are likely related. Ni-bearing sulfides and arsenides predominate; pentlandite is the most common sulfide, but millerite associated with magnetite, maucherite, gersdorffite and Bi-sulfides is present in all the PGE-bearing ultramafic rock-types, including the chromitite, serpentinite with disseminated chromite and the chromite-poor, sulfide-bearing serpentinite. The sulfides and arsenides commonly form composite grains attached to the edges of chromite grains and are typically partially surrounded by serpentine. Pentlandite is commonly partially altered to millerite and magnetite. Gersdorffite and maucherite occur on the edges of the

pentlandite – millerite – magnetite aggregates. Maucherite, poorly crystalline and with a mottled appearance, locally replaces pentlandite (Fig. 10). Typical compositions of the sulfides and arsenides are given in Table 5.

In the PGE-enriched sulfide-bearing serpentinite, pentlandite is more abundant than in the other lithologies, with maucherite, gersdorffite and minor millerite also present. In this lithology, however, they are joined by nickeloan pyrrhotite, pyrrhotite, pyrite, chalcopyrite, minor Zn and Pb sulfides and ilmenite. Pentlandite and pyrrhotite occur together, and nickeloan pyrrhotite forms laths within the pentlandite. Rarely, pentlandite is partially altered to millerite with euhedral pyrite (Fig. 11).

An additional sulfide assemblage is present in PGM-bearing chlorite-filled veins that cross-cut both chromite and serpentine. These veins contain an arsenic-poor assemblage of chalcopyrite, pentlandite and a Co-bearing pentlandite (too small for analysis, but which is probably cobaltian pentlandite). Adjacent to the chromite grains, the chlorite in the veins is Cr-bearing (1–1.5%), whereas a few tens of μm away from the chromite grain, the chlorite in the veins is barren of Cr.

PLATINUM-GROUP MINERALS IN NON-LATERITIZED SAMPLES

All six PGE have been observed as major components of PGM in these samples. The most common minerals include Pd bismuthides, sperrylite, laurite and irarsite. The PGM are typically subrounded and form composite grains that are less than $10\ \mu\text{m}$ in diameter. They are commonly associated with sulfides and arsenides surrounded by chromite and serpentine. Plati-

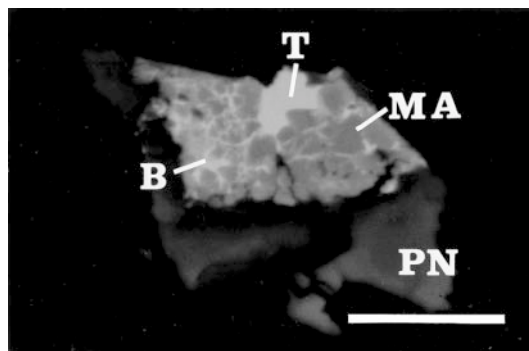


FIG. 10. Back-scattered scanning electron microscope image of a composite grain of pentlandite (PN) partially replaced by a mottled grain of maucherite (MA) hosting a grain of Pd–Bi telluride (T) and Pd bismuthides (B) filling interstitial spaces between the maucherite grains. This composite grain is surrounded by serpentine. Sample BC 104 (Table 2). Scale bar represents $5\ \mu\text{m}$.

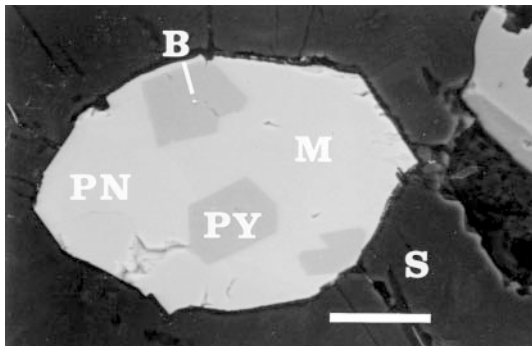


FIG. 11. Back-scattered scanning electron microscope image of a composite grain of Ni-Fe sulfides surrounded by serpentine (S). Pentlandite (PN) is partially altered to millerite (M), and the millerite hosts euhedral crystals of pyrite (PY), the largest of which contains a 1–2 μm grain of Pd bismuthide (B). Sample PT18 (Table 2). Scale bar represents 20 μm .

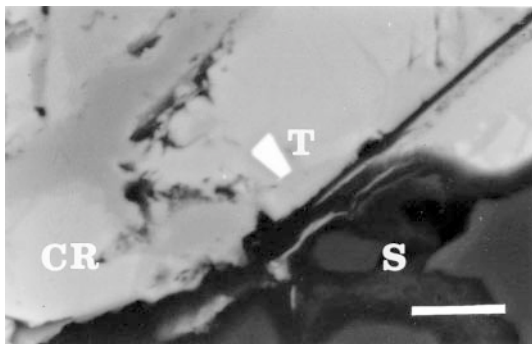


FIG. 12. Back-scattered scanning electron microscope image of an euhedral crystal of Pd-Bi telluride (T) surrounded by mottled and altered chromite on the margin of the grain (CR) near its contact with silicate (S). Sample BC104 (Table 2). Scale bar represents 5 μm .

num-group minerals also occur in the cross-cutting chlorite-rich veins.

Samples of chromitite, serpentinite with disseminated chromite and sulfide-bearing serpentinite were all examined for PGM. Distinct differences were found in the PGM assemblages in each rock type. The PGM assemblage in the chromitite is dominated by Os-, Ir-, Ru as well as Pd-, Rh- and Pt-bearing minerals, whereas Os- Ir- and Ru-bearing PGM are rare in the chromite-poor serpentinite, as reflected in the whole-rock concentrations of the PGE. Only in the sulfide-bearing serpentinites is sperrylite common.

Bismuthides of palladium are ubiquitous in the PGE-bearing samples; they vary from 0.5 to 6 μm in diam-

eter and are locally Te-bearing. They typically occur as discrete grains in the vein assemblage, in which elongate Te-poor Pd bismuthides dominate, but in chromitite they are associated with laurite and irarsite, and in the sulfide-bearing serpentinite, they occur with sperrylite. The only Pd bismuthides large enough to quantitatively analyze are michenerite and sobolevskite (anal. 1–3, Table 6). Pd bismuthides occur in a number of textural sites associated with base-metal sulfides and arsenides, especially where pentlandite is partially altered. Thus, they tend to be located on the edge of pentlandite grains that are being replaced by millerite and magnetite. In several cases, Pd bismuthides form tiny (1–2 μm) rounded grains in euhedral pyrite surrounded by millerite, which incompletely replaces pentlandite (Fig. 11). Palladium bismuthides also occur as rounded grains enclosed by minerals such as maucherite, gersdorffite and nickeloan pyrrhotite, located on the edge of pentlandite. Maucherite on the edge of pentlandite may appear mottled, suggesting that it is inhomogeneous. Palladium-bismuth telluride grains in the maucherite are hosted by Pd bismuthides that infill interstitial irregular elongate spaces in the granular texture. Rarely are the Pd bismuthides enclosed by chromite, but they do occur within an altered zone at the edge of the chromite close to the adjacent serpentine (Fig. 12), and in one case an elongate Pd bismuthide occurs at the junction of ilmenite and serpentine. Other Pd-bearing minerals are much less common, but Pd bismuthides locally form rounded grains with Pd arsenides, sulfarsenides and antimonides. In one case, a euhedral grain of gersdorffite totally enclosed in pentlandite is partially surrounded and is probably being replaced; the mottled zone seems to be a mixture of maucherite and gersdorffite. Elongate lenses of Pd-bearing PGM are located at the junctions of this mottled zone, both with the gersdorffite and surrounding pentlandite (Fig. 13). These Pd-bearing minerals are too small for quantitative analysis. Analysis of these minerals for trace concentrations of Pt and Pd revealed up to 0.18% Pd in the gersdorffite, whereas Pt was below the detection limit of 0.05%. Mapping showed that the maximum Pd concentration was in the center of the gersdorffite, suggesting that the source of the Pd for the adjacent Pd-bearing PGM in the maucherite was the gersdorffite and that the Pd was being removed preferentially from the edge of the gersdorffite. Pentlandite, millerite and pyrite were also analyzed for traces of Pt and Pd, but neither was detected in any of these minerals.

Locally, the Pd bismuthides occur in silicate-filled veins that cross-cut both serpentine, and rarely, the chromite grains (Figs. 14, 15). The veins are 50–100 μm in length, only 1–2 μm wide and are irregular and jagged, suggesting that they formed during late, low-temperature, brittle fracturing. They can occur in an *en échelon* arrangement of several veinlets, and in some cases emanate from sulfides into the surrounding serpentine. The Pd bismuthides may attain 20 μm in length

TABLE 6. COMPOSITIONS OF THE PGM FROM THE BACURI COMPLEX, NORTHEASTERN BRAZIL.

Grain no.	1	2	3	4	5	6	7	8	9	10
Sample no.	BC 12	BC 104	BC 65	PT 5	PT 5	PT 5	BC 12	BC 104	BC 12	BC 104
Ru wt%				37.3	54.9	0.7	4.4	1.6		
Rh						0.8		28.5		
Pd	22.4	32.9	34.6							
Os				22.7	1.6		33.6	4.2		
Ir				3.1	1.5	58.4		2.5		
Pt						2.2		17.4	55.4	54.9
Cr	(1.6)	(1.4)	(1.0)	(0.7)	(0.6)	(0.9)		(1.5)	(0.3)	
Fe	(2.0)	(1.0)	(0.5)	0.8	0.7	(0.7)	(3.5)	(1.2)	(1.5)	(2.1)
Ni				1.4	(4.6)	(14.7)	(0.4)			
As				1.5	22.4	29.6	32.9	41.4	41.5	
Bi	45.7	57.0	41.1							
Te	28.2	5.1	19.9							
S		3.8	2.3	34.5	37.5	10.5	13.0	11.7		
Sb										
total	99.9	99.8	100.2	99.4	99.8	100.9	99.7	100.4	99.8	98.8

Name	Formula	Size (μm)	Mineral associations
1 Michenerite	$\text{Pd}_{0.97}\text{Bi}_{1.01}\text{Te}_{0.02}$	4.5×4.5	Silicate in chromite
2 Sobolevskite	$\text{Pd}_{0.95}(\text{Bi}_{0.83}\text{Te}_{0.12}\text{Sb}_{0.10}\text{S}_{2.10})$	6×6	Silicate + nickeloan pyrrhotite
3 Sobolevskite	$\text{Pd}_{0.94}(\text{Bi}_{0.14}\text{Te}_{0.41}\text{Sb}_{0.03}\text{S}_{2.10})$	30×30	Chromite, Ni sulfide and silica
4 Laurite	$(\text{Ru}_{0.70}\text{Os}_{0.23}\text{Ir}_{0.02}\text{S}_{2.96})$	20×8	Chromite and Ir-AsS inclusions
5 Laurite	$(\text{Ru}_{0.64}\text{Os}_{0.01}\text{Ir}_{0.01}\text{S}_{2.02})$	6×3.7	Chromite, NiAsS and NiS
6 Irsite	$(\text{Ir}_{0.95}\text{Pt}_{0.04}\text{Ru}_{0.02}\text{Rh}_{0.02}\text{S}_{2.01})$	3×2	Inclusion in laurite
7 Osarsite	$(\text{Os}_{0.99}\text{S}_{1.01})$ ideally $(\text{Os,Ru})\text{AsS}$, with matrix contributions (As, S)	1.7×1	In Ni-Fe sulfarsenide
8 Hollingworthite	$(\text{Rh}_{0.76}\text{Pt}_{0.24}\text{Os}_{0.06}\text{Ru}_{0.04})$	20×5	Silicate + nickeloan pyrrhotite
9 Sperrylite	$\text{Pt}_{1.02}\text{As}_{1.08}$	2.5×2.5	Chromite and silicate
10 Sperrylite	$\text{Pt}_{1.01}\text{As}_{1.09}$	4×4	Silicate and pentlandite

Concentrations of Cr, Fe and Ni enclosed in brackets are attributed to excitation in minerals surrounding the PGM. These values have not been used in the calculation of formulas.

and occur as elongate minerals with rounded ends oriented, with the long axis parallel to the long axis of the vein. They may be accompanied by chalcopyrite, magnetite and, rarely, Co-bearing pentlandite. Elongate Pd bismuthides and chalcopyrite also occur in chlorite adjacent to chromite grains, and these PGM are oriented along the prominent cleavage of chlorite (Fig. 16).

The most common PGM in the chromitite are laurite and irrsite. These are accompanied by smaller grains of Pd bismuthides. Laurite and irrsite are commonly subhedral and rarely euhedral. They form composite grains 2 to 25 μm in diameter in which the laurite tends to surround irrsite. Laurite is either pure or contains minor Os and Ir, and the irrsite is either pure or contains traces of Rh or Pt (anal. 4, 5 and 6 in Table 6). Composite grains of laurite and irrsite commonly lie either at margins of chromite grains adjacent to silicate, or at the boundary between chromite crystals (Figs. 17,

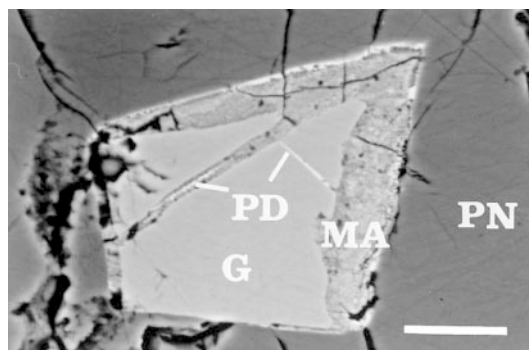


FIG. 13. Back-scattered scanning electron microscope image of euhedral gersdorffite (G) surrounded by pentlandite (PN) and rimmed and veined by maucherite (MA). Lozenge-shaped grains of Pd-Ni-Fe-As-S (PD) occur within the maucherite vein crossing the gersdorffite and at the junction between the maucherite and pentlandite. We contend that the PGM formed as alteration of the gersdorffite occurred, the Pd unable to be retained within the maucherite. Sample PT18 (Table 2). Scale bar represents 10 μm .

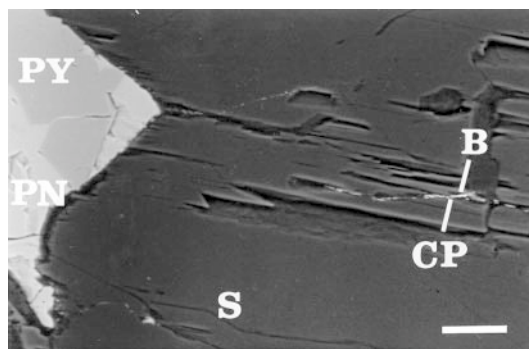


FIG. 14. Back-scattered scanning electron microscope image of a series of subhorizontal parallel veins in serpentine (S) containing Pd bismuthide (B) accompanied by an elongate grain of chalcopyrite (CP). A grain of pentlandite (PN) is partially altered to pyrite (PY). The veins containing Pd and Cu-bearing minerals are evidence for the late-stage remobilization of Pd and Cu. Sample PT18 (Table 2). Scale bar represents 20 μm .

18). Platinum-group minerals within the euhedral chromite grains are rare; only one grain of laurite was found enclosed in chromite. Laurite and irrsite are also located at the edge of pentlandite grains associated with millerite and minor maucherite. Where associated with Pd bismuthides, laurite and irrsite occur adjacent to or very close to each other, typically surrounded by and near the edge of millerite grains (Fig. 19).

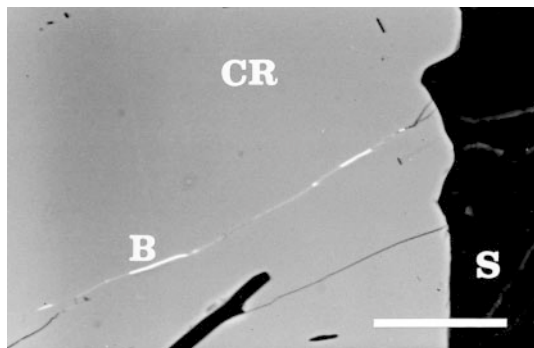


FIG. 15. Back-scattered scanning electron microscope image of a vein filled with a Pd bismuthide (B) cross-cutting chromite (CR). Sample PT18 (Table 2). Scale bar represents 20 μm .

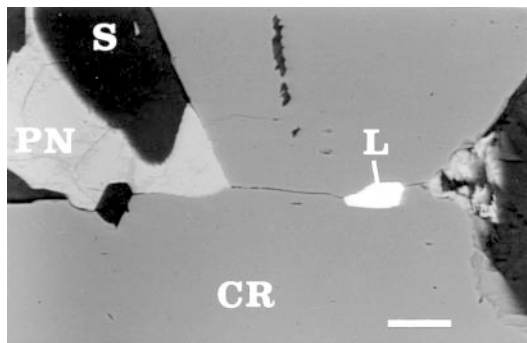


FIG. 17. Back-scattered scanning electron microscope image of a composite grain of laurite and irarsite (L) at the junction of two crystals of chromite (CR) located in silicate (S) and containing pentlandite altering to millerite (PN). Sample PT5 (Table 2). Scale bar represents 20 μm .

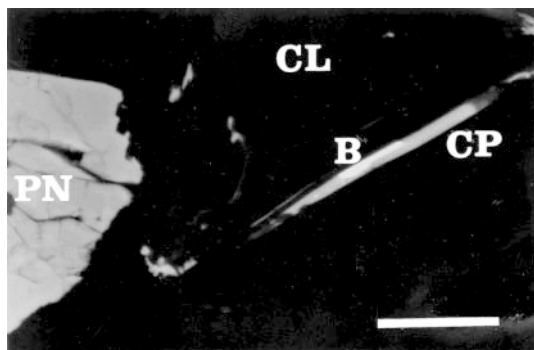


FIG. 16. Back-scattered scanning electron microscope image showing elongate grain of chalcopyrite (CP) and a Pd bismuthide (B) in serpentine, enclosed by chromian chlorite and oriented parallel to the cleavage of the chlorite (CL), near a grain of pentlandite (PN). Sample BC104 (Table 2). Scale bar represents 10 μm .

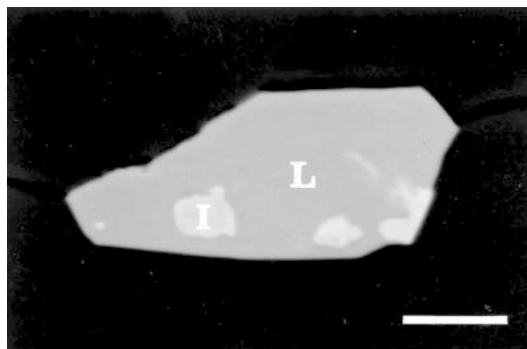


FIG. 18. Back-scattered scanning electron microscope image of an enlarged part of Figure 17 illustrating the subhedral nature of the laurite (L) (anal. 4, Table 6) surrounding subhedral irarsite (I) (anal. 6, Table 6). Sample PT5 (Table 2). Scale bar represents 5 μm .

Sperrylite is the most abundant Pt-bearing mineral in the sulfide-bearing serpentinite, as solitary euhedral or subhedral crystals, 1–5 μm in diameter, commonly hosted by silicate. Only in one case was sperrylite observed near the edge, but totally enclosed in, homogeneous chromite, an accessory mineral within the serpentinite. Other Pt-bearing minerals are rare, but Pt occurs in hollingworthite and in one irregularly shaped grain of Pt telluride, smaller than 1 μm , hosted by pentlandite.

In samples containing disseminated crystals of chromite in serpentine, the PGM assemblage consists of Os-, Ir-, Ru-, and Pt-bearing minerals, in addition to the ubiquitous Pd bismuthides. In one such sample, a pentlandite grain is partially altered to mottled, inhomogeneous maucherite and contains a 1- μm grain interpreted to be osarsite (Os,Ru)As₂S₂ (anal. 7, Table 6),

although the grain contains high levels of As and S, probably derived from the surrounding maucherite matrix. The PGM in this sample are not abundant but reflect both the Pt-rich PGM assemblage of the sulfide-bearing serpentinite, characterized by sperrylite, and the PGM assemblage of the massive chromitite, characterized by Os-, Ru-, and Ir-bearing minerals.

DISCUSSION

Composition of chromite

Chromitite in continental layered complexes usually forms regular layers which at certain stratigraphic horizons extend over much of the area of the layered complex, whereas in ophiolite complexes the chromitite is

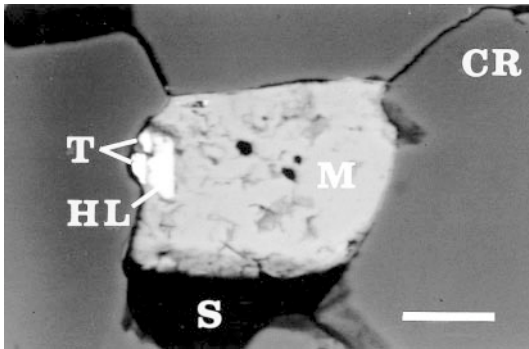


FIG. 19. Back-scattered scanning electron microscope image showing a cluster of PGM on the edge of an inclusion of millerite (M) with minor silicate (S) and surrounded by chromite (CR). Te-bearing Pd bismuthides (T) form two irregularly shaped crystals nearest to the edge of the millerite, and close to these is a composite grain of hollingworthite enclosed by laurite (HL). Sample PT5 (Table 2). Scale bar represents 10 μm .

laterally discontinuous and podiform in shape (*e.g.*, Roberts & Neary 1993). In the Bacuri complex, the chromitite layers are so deformed that the original geometry is difficult to reconstruct. However, it has been

known for a long time that chromite grains in layered complexes usually are euhedral, whereas in ophiolites, the high-temperature shearing associated with ocean spreading leads to a predominance of irregular, deformed and rounded grains (Thayer 1960). In the Bacuri complex, despite the striking deformation of the layers, the chromite crystals are dominantly euhedral, suggesting that Bacuri is a layered complex that crystallized in a tectonically quiet regime.

The magmatic composition of chromite from layered complexes and the different types of ophiolitic complexes is distinctly different. Discrimination diagrams that define specific compositional fields of chromite have been constructed by several authors, among them Dickey (1975) and, more recently, Stowe (1994) and Roeder (1994). The Bacuri chromitites show compositional trends that generally fall outside the fields of massive chromitite for both layered and ophiolite complexes (Figs. 20–23), probably because of the extensive alteration of the complex during serpentinization. The effects of such alteration are well known; they will cause an increase in Fe^{3+} at the expense of Al (Evans & Frost 1975), and Fe^{2+} will increase at the expense of Mg (Jan *et al.* 1985).

The Bacuri chromitite has been pervasively altered, with chromite grains having uniform compositions. The $\text{Mg}/(\text{Mg} + \text{Fe}^{2+})$ value may be low owing to the alteration of the Bacuri complex (Fig. 20). Similarly, Stowe

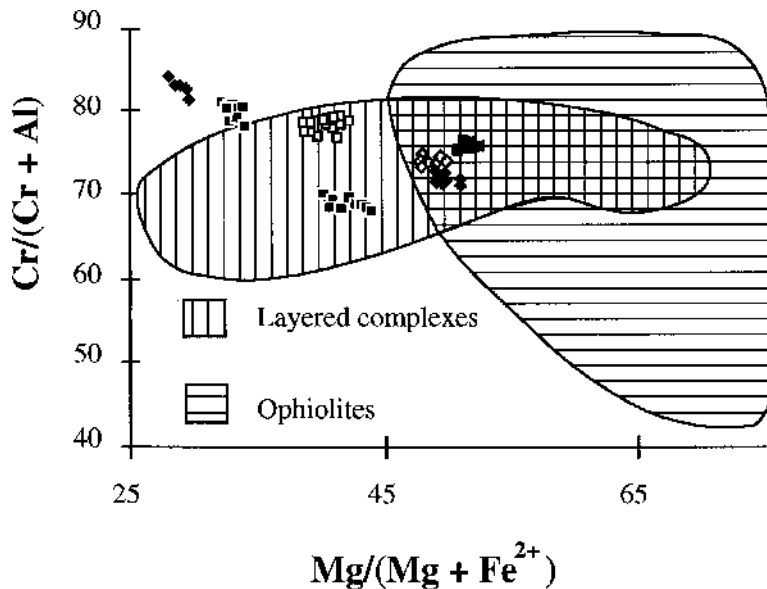


FIG. 20. $\text{Cr}/(\text{Cr} + \text{Al})$ versus $\text{Mg}/(\text{Mg} + \text{Fe}^{2+})$ showing the distribution of chromite compositions at Bacuri compared with fields for layered and ophiolite complexes, after Stowe (1994). The compositions have different symbols corresponding to chromitites from different localities shown in Figure 1. Black squares represent B1, open squares, B5, black diamonds, C5, and open diamonds, Samaca.

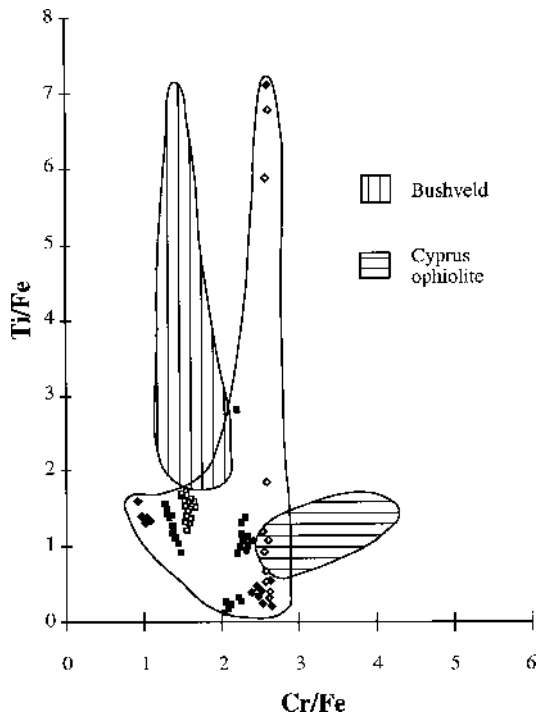


FIG. 21. Ti/Fe versus Cr/Fe showing the distribution of chromite compositions at Bacuri compared with fields for the Bushveld complex as an example of layered complexes, and Cyprus as an example of ophiolite complexes, after Neary & Brown (1979). The key to the symbols is given in the caption to Figure 20.

(1994) noted that the maximum Cr:Fe ratio for ophiolite complexes is usually higher (greater than 3) than for layered complexes, but alteration may lower this ratio (Fig. 21). Alteration could account also for the high $\text{Fe}^{2+}:\text{Mg}$ ratio of the samples (Fig. 22) and could be responsible for the high Fe^{3+} and low Al values of the Bacuri chromitite (Fig. 23). Another characteristic of chromitite from layered complexes is the higher Ti than in ophiolites. Jan *et al.* (1985) noted that Ti in chromite from ophiolites may increase in ferric chromite rims during alteration of chromite. However, the highest values they quoted in rims or centers of their chromite is 0.31% TiO_2 . The Bacuri chromites have higher TiO_2 values, with three grains containing 1.69, 1.45 and 1.66%. These values occur in three different samples, each from different localities, and may be due to alteration. However many of the compositions of chromite grains from the Bacuri complex have Ti values greater than 0.31% TiO_2 (Fig. 22). Such compositions of the chromite, taken in conjunction with the other textural evidence, suggest that the Bacuri complex has a stratiform, continental rather than ophiolitic origin.

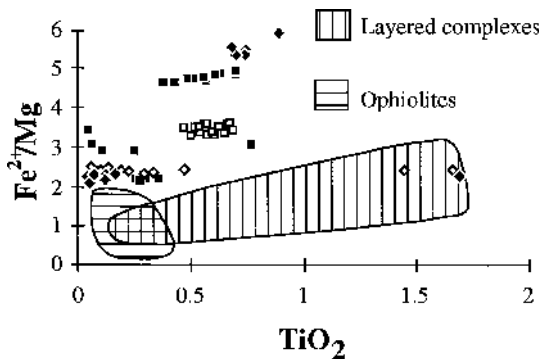


FIG. 22. $\text{Fe}^{2+}:\text{Mg}$ versus TiO_2 showing the distribution of chromite compositions at Bacuri compared with fields for layered and ophiolite complexes, after Dickey (1975). The key to the symbols is given in the caption to Figure 20.

Further work is needed to determine the variation in chromite compositions throughout the complex to further understand the fractionation of the chromite and the tectonically complicated relationship among the chromitite bodies. However, the composition of the chromite has a limited range of Cr content both from different parts of the complex and within the one layer from GS295, indicating a lack of extreme magmatic fractionation during crystallization. Open-system fractionation during crystallization with replenishment of the magma chamber (*e.g.*, Naslund & McBirney 1996) could be a way to achieve this constancy.

Igneous concentration of the PGE

Magmatic associations of the PGE may be divided into Os, Ir and Ru, commonly concentrated within chromitite (von Gruenewaldt *et al.* 1986, Constantinides *et al.* 1980, Talkington *et al.* 1984, Augé 1986, Lee 1996), and Pt, Pd and Rh, concentrated with sulfides (Naldrett & Duke 1980). If sulfur saturation occurs as chromite crystallizes, then Pt, Pd and Rh are also concentrated with sulfides in the chromitite (Gain 1985, Hiemstra 1985). In the Bacuri complex, the PGE-enriched, sulfide-bearing serpentinite has a positive chondrite-normalized PGE signature, with enrichment in Pt and Pd, a pattern typical of PGE enrichment with sulfides (Fig. 7). In contrast, the chromitites and the serpentinite with disseminated chromite have a pattern with a positive Ru anomaly typical of massive chromitite, and may have a positive slope from Pt to Pd typical of chromitites containing sulfides.

The PGM assemblage in the Bacuri complex reflects the whole-rock PGE concentrations, with Os, Ir and Ru minerals restricted to the chromitite, and Pt, Pd and Rh minerals associated with both sulfides in the chromitite and in the sulfide-bearing serpentinite. In the chromitite,

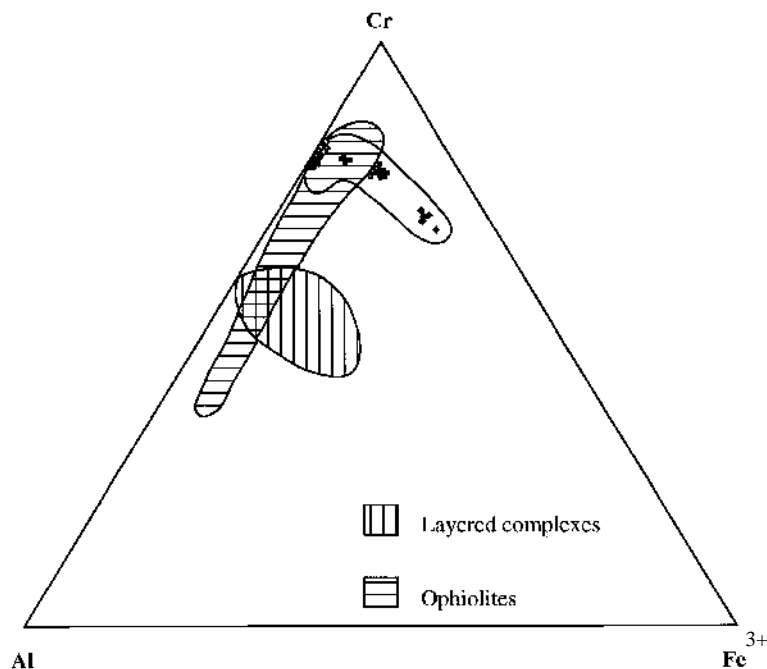


FIG. 23. Triangular diagram of Cr–Al–Fe³⁺ showing the distribution of chromite compositions at Bacuri compared with fields for layered and ophiolite complexes, after Dickey (1975). The key to the symbols is given in the caption to Figure 20.

all the PGM tend to occur together with the laurite, and are commonly spatially associated with pentlandite and its alteration products of Ni arsenides, millerite and Pd–Bi tellurides. This distribution of PGM associated with chromite has been observed in both ophiolite complexes (Prichard *et al.* 1994) and layered complexes (Viljoen *et al.* 1986a), especially in the Bushveld (Lee 1996), where Os-, Ir- and Ru-dominant alloys are interpreted to have crystallized prior to chromite crystallization; Pt-, Pd- and Rh-dominant minerals crystallized over a longer period and continued to crystallize later than the Os-, Ir- and Ru-dominant phases. Thus, the original igneous distribution of the PGE within the chromitite and serpentinite in the non-lateritized parts of the Bacuri complex is largely preserved, with Os, Ir and Ru concentrated with chromitite, and Rh, Pt and Pd with disseminated sulfides.

Secondary PGM

The complex has been extensively altered, with widespread serpentinization and a sulfide–sulfarsenide assemblage of millerite, pyrite, gersdorffite and maucherite. All the host primary PGE-bearing minerals are considered to have been modified by this alteration. It is not possible to determine whether the PGE were origi-

nally concentrated in solid solution in sulfides or if they formed primary PGM, but the association of PGM with the altered sulfides certainly suggests that the PGM and sulfides crystallized together. Palladium is known to be concentrated in magmatic sulfides, especially pentlandite, and expelled during cooling and alteration of these sulfides (Cabri 1992, Czamanske *et al.* 1992, Li *et al.* 1993). This pattern agrees with the experimental work of Makovicky *et al.* (1990). In the Bacuri samples, the Pd may have been originally held in solid solution in the pentlandite; this phase is partially or totally altered to millerite and magnetite, and the Pd-bearing PGM occur as rounded grains in these alteration minerals. The pentlandite has been altered during serpentinization and no longer contains detectable traces of Pt or Pd. In addition, in the sulfide-bearing serpentinite, pentlandite occurs with pyrrhotite, and Pd bismuthide is concentrated along the edges of both minerals with exsolved nickeloan pyrrhotite. Euhedral pyrite, with undetectable Pt or Pd, is hosted by millerite after pentlandite, and in several cases Pd bismuthide is found as tiny (1–2 μm), rounded grains within this pyrite. Inhomogeneous mottled maucherite also is a common product of alteration of the pentlandite and contains Pd bismuthide that forms discrete PGM, either as round or elongate crystals, along the margins of the arsenide grains.

The occurrence of gersdorffite as a PGE host has been described elsewhere; Pt and Rh (Prichard *et al.* 1994) and Rh and Pd (Barkov *et al.* 1996, Cabri 1992) have been observed in solid solution in gersdorffite. The Pd in the gersdorffite may have been derived from pentlandite. Pd held in solid solution in the gersdorffite is likely to have been released during alteration to maucherite to form Pd bismuthides within the maucherite. Thus in some cases, the Pd may have been hosted by pentlandite, now barren of Pt or Pd, gersdorffite and then PGM.

The Os-, Ir- and Ru-bearing PGM also represent an alteration assemblage. Tarkian & Prichard (1987) suggested that laurite and irarsite occur together upon alteration of the Ir-bearing laurite and the associated introduction of As. Similarly, composite laurite and irarsite grains occur in the Bacuri complex and are commonly associated with sulfides and Pd-bearing minerals, possibly the result of magmatic processes that concentrated these PGE and sulfides together.

The predominant PGM assemblages in layered intrusions tend to include both Pt and Pd sulfides and Pt and Pd bismuthides, tellurides and arsenides (Viljoen *et al.* 1986b, Volborth *et al.* 1986). In some cases, these bismuthides, tellurides and arsenides may be primary (Genkin & Evstigneeva 1986, Czamanske *et al.* 1992, Li *et al.* 1992), whereas other authors have suggested that PGM may be modified during alteration to produce bismuthides, tellurides and arsenides (Prichard *et al.* 1994, Corrivaux & Laflamme 1990, Thalhammer & Stumpfl 1988). In complexes where the PGE concentrations are predominantly associated with chromitite rather than massive sulfide, primary magmatic Pt and Pd sulfides are dominant over bismuthides and tellurides, as in giant layered complexes such as the Bushveld (Kinloch 1982) and in smaller complexes such as Cabo Ortegal (Moreno *et al.* 1999). Pt or Pd sulfides have not been observed during this initial study of the PGM in the Bacuri complex. In complexes that are so extensively altered, it is difficult to demonstrate whether the bismuthides, tellurides and arsenides are primary or secondary, replacing Pt- and Pd-bearing sulfides formed either directly from the magma or during expulsion from base-metal sulfides on cooling or during an earlier stage of alteration.

Mobilization of the PGE

Traditionally, the PGE have been considered to be immobile, but their mobility has been debated. Hydrothermal PGE mineralization has been proposed for the Cu-Ni sulfide occurrence at Rathbun Lake, northeastern Ontario (Rowell & Edgar 1986) and for the New Rambler mine in Wyoming (McCallum *et al.* 1976). Pd is known to be more mobile than Pt, especially during weathering (Fuchs & Rose 1974, Prichard & Lord 1994). This mobility is corroborated by experimental results (Mountain & Wood 1987, 1988, Evstigneeva & Tarkian 1996) showing that PGE are capable of being

mobilized in hydrothermal solutions. In the Bacuri samples, local postmagmatic remobilization of the Pd from host sulfides is unusually clearly demonstrated by the presence of Pd bismuthides in veins that cross-cut grains of chromite and serpentine. Chlorite (chromian near chromite grains) is the dominant silicate in these veins. Chlorite is commonly described as an alteration mineral formed during serpentinization, with Al and Cr derived from alteration of the chromite grains (Ulmer 1974, Jan *et al.* 1985). The occurrence of chlorite and Pd bismuthides in these veins indicates the mobilization of Pd to form PGM during the process of serpentinization and the associated alteration of the chromite. These Pd-rich PGM occur with chalcopyrite in the veins, suggesting contemporary mobilization of Pd with Cu and reprecipitation. These PGM in the Bacuri samples demonstrate the mobility of Pd in the initial stages of mobilization, where it is still possible to relate the secondary PGM to their PGE source in the altered sulfide host only a few micrometers away.

Chondrite-normalized PGE patterns for Os, Ir, Ru, Rh and Pt preserve igneous patterns, with Ru-enriched patterns for chromitite and positive Pt-rich patterns for sulfide-bearing serpentinite. The slope between Pt and Pd varies from positive to negative owing to variations in Pd concentration. Positive slopes are typical of sulfide-bearing magmatic patterns, whereas negative slopes probably indicate Pd removal associated with possible remobilization (Fig. 7). Magmatic Pt:Pd ratios tend to be fairly constant, and commonly less than 1 (Cabri 1989). During alteration, however, Pd has been found to be more mobile than Pt (Fuchs & Rose 1974, Prichard & Lord 1994). The Pt:Pd values in the Bacuri samples are less variable in the chromitite than in the samples of serpentinite with disseminated chromian spinel, and in sulfide-bearing serpentinite where Pd bismuthide in veins is most common. The lower Pt:Pd ratios are in some cases associated with high Cu, and correspond to the mineralogical association of chalcopyrite and Pd-bearing PGM, especially in veins (Fig. 8). These lower Pt:Pd values reflect the original magmatic values; although the Pd has been mobilized into veins a few micrometers from their source, the whole-rock composition of these samples includes the Pd in the veins. Higher Pt:Pd ratios tend to occur where both Pt and Pd values are low and the Cu concentration also is low.

Lateritization

Laterites developed on ultramafic rocks have been studied for their potential value in the concentration of Ni. Laterites with a limonitic zone and an underlying saprolitic zone are described from humid tropical areas where leaching is extensive and Ni is enriched in the saprolitic zone (Golightly 1981). Comparisons of typical compositions of limonitic, saprolitic and host fresh rock for New Caledonia (Troly *et al.* 1979) and for Niquelandia, Brazil (Colin *et al.* 1990) show that Fe, Al

and Cr increase in the limonitic zone relative to the lower zones, and Ni and Co tend to be leached compared to the underlying saprolitic zone but are approximately the same as in the bedrock. In the Bacuri laterites, the tropical climate, with high rainfall and no marked dry season, has produced a depletion in Co, Ni and Cu in the limonitic zone compared with the bedrock and a steady increase in Ni downward through the saprolitic zone into the bedrock. No enrichment in Ni was observed in the saprolitic zone in this study. Despite this high degree of leaching, Pt has been retained in one sample of Cr-rich limonite. The Pt:Pd value for this sample is much higher than in the saprolitic zone and underlying non-lateritized ultramafic rock, and indicates retention of Pt and possible extensive removal of Pd.

CONCLUSIONS

The chromian spinel shows low Mg/Fe²⁺ values and a low Al content, suggestive of pervasive alteration during serpentinization, but the high Ti values, although possibly enhanced by alteration, together with the euhedral shape of the chromite grains, are characteristic of layered igneous complexes. A geochemical traverse of chromite compositions across one of the thick layers of chromitite showed no systematic variation, possibly indicating an open-system crystallization with constant replenishment of relatively Cr-rich magma. Pt and Pd are not systematically concentrated in the chromitites, but are enriched sporadically with minor precipitation of sulfide. Os-, Ir- and Ru-bearing PGM have been located in PGE-bearing chromitite and include laurite, irarsite and Pd bismuthides, whereas in sulfide-bearing serpentinite, the PGM are dominated by Pt, Pd and Rh minerals, mainly sperrylite, hollingworthite and Pd bismuthides. The PGM are part of an alteration assemblage with secondary silicates and sulfides. Bismuthides of Pd in some cases occur within pyrite associated with millerite after pentlandite and in veins that cross-cut aggregates of sulfide minerals. The Pd is interpreted as having been partially remobilized, and the host minerals, recrystallized tens of micrometers from their source in magmatic sulfides, altered during serpentinization. Cobalt, Ni and Pd have been leached during laterite formation to a depth of 10 meters, but Pt is conserved.

ACKNOWLEDGEMENTS

We are happy to dedicate our paper to Peter Roeder, who has contributed significantly throughout his career to our understanding of the geochemistry of chromian spinel in various tectonic environments. We thank the Caemi Mining Group for allowing us access to the site, and Carlos Alberto Spier for help in finding our way around the hundreds of boxes of drill core. We also thank Eric Condliffe for analysis of the chromite grains. Drs. Catharine Farrow and Mike Zientek are thanked

for their constructive and detailed reviews, and Professor Robert F. Martin for his usual careful editing.

REFERENCES

- AUGÉ, T. (1986): Platinum-group mineral inclusions in chromitites from the Oman ophiolite *Bull. Minéral.* **109**, 301-304.
- BARKOV, A.Y., ALAPIETI, T., LAAJOKI, K. & PEURA, R. (1996): Osmian hollingworthite and rhodian cobaltite-gersdorffite from the Lukkulaivaara layered intrusion, Russian Karelia. *Mineral. Mag.* **60**, 973-978.
- CABRI, L.J. (1981): Platinum-group elements: mineralogy, geology, recovery. *Can. Inst. Mining Metall., Spec. Vol.* **23**.
- _____ (1992): The distribution of trace precious metals in minerals and mineral products. *Mineral. Mag.* **56**, 289-308.
- COLIN, F., NAHON, D., TRESCASES, J.J. & MELFI, A.J. (1990): Lateritic weathering of pyroxenites at Niquelandia, Goias, Brazil: the supergene behaviour of nickel. *Econ. Geol.* **85**, 1010-1023.
- CONSTANTINIDES, C.C., KINGSTON, G.A. & FISHER, P.C. (1980): The occurrence of platinum-group minerals in the chromitites of the Kokkinorotsos chrome mine, Cyprus. *In Ophiolites* (A. Panayiotou, ed.). Proc. Int. Ophiolite Symp. (Cyprus, 1979). Ministry of Agriculture and Natural Resources, Nicosia, Cyprus (93-101).
- CORRIVAUX, L. & LAFLAMME, J.H.G. (1990): Minéralogie des éléments du groupe du platine dans les chromitites de l'ophiolite de Thetford Mines, Québec. *Can. Mineral.* **28**, 579-595.
- CZAMANSKE, G.K., KUNILOV, V.E., ZIENTEK, M.L., CABRI, L.J., LIKHACHEV, A.P., CALK, L.C. & OSCARSON, R.L. (1992): A proton-microprobe study of magmatic sulfide ores from the Noril'sk-Talnakh district, Siberia. *Can. Mineral.* **30**, 249-287.
- DE MONTALVÃO, R.M.G. & TASSINARI, C.C.G. (1984): Geocronologia Pré-Cambriana do Território Federal do Amapá (Brazil). *In Symp. Amazonico II* (Manaus), 53-57.
- DICKEY, J.S., JR. (1975): A hypothesis for the origin of podiform chromite deposits. *Geochim. Cosmochim. Acta* **39**, 1061-1074.
- EVANS, B.W. & FROST, B.A. (1975): Chrome spinel in progressive metamorphism – a preliminary analysis. *Geochim. Cosmochim. Acta* **39**, 959-972.
- EVSTIGNEVA, T. & TARKIAN, M. (1996): Synthesis of platinum-group minerals under hydrothermal conditions. *Eur. J. Mineral.* **8**, 549-564.
- FUCHS, W.A. & ROSE, A.W. (1974): The geochemical behaviour of platinum and palladium in the weathering cycle in the Stillwater complex, Montana. *Econ. Geol.* **69**, 332-346.

- GAIN, S.B. (1985): The geologic setting of the platiniferous UG-2 chromitite layer on the farm Mandaagshoek, eastern Bushveld Complex. *Econ. Geol.* **80**, 925-943.
- GENKIN, A.D. & EVSTIGNEVA, T.L. (1986): Associations of platinum-group minerals of the Noril'sk copper-nickel sulfide ores. *Econ. Geol.* **81**, 1203-1212.
- GOLIGHTLY, J.P. (1981): Nickeliferous laterite deposits. *Econ. Geol.*, 75th Ann. Vol., 710-735.
- HIEMSTRA, S.A. (1985): The distribution of some platinum-group elements in the UG2 chromitite layer of the Bushveld complex. *Econ. Geol.* **80**, 944-957.
- JAN, M.Q., WINDLEY, B.F. & KHAN, A. (1985): The Waziristan ophiolite Pakistan: general geology and chemistry of chromite and associated phases. *Econ. Geol.* **80**, 294-306.
- KINLOCH, E.D. (1982): Regional trends in the platinum-group mineralogy of the critical zone of the Bushveld complex, South Africa. *Econ. Geol.* **77**, 1328-1347.
- LEE, C.A. (1996): A review of mineralisation in the Bushveld complex and some other layered intrusions. In *Layered Intrusions* (R.G. Cawthorn, ed.). Elsevier, Amsterdam, The Netherlands (103-147).
- LI, CHUSI, NALDRETT, A.J., COATS, C.J.A. & JOHANNESSEN, P. (1992): Platinum, palladium, gold and copper-rich stringers at the Strathcona mine, Sudbury: their enrichment by fractionation of a sulfide liquid. *Econ. Geol.* **87**, 1584-1598.
- _____, _____, RUCKLIDGE, J.C. & KILIUS, L.R. (1993): Concentrations of platinum-group elements and gold in sulfides from the Strathcona deposit, Sudbury, Ontario. *Can. Mineral.* **31**, 523-531.
- MAKOVICKY, E., KARUP-MØLLER, S., MAKOVICKY, M. & ROSE-HANSEN, J. (1990): Experimental studies on the phase systems Fe-Ni-Pd-As-S applied to PGE deposits. *Mineral. Petrol.* **42**, 307-319.
- MATOS, A.A. DE, SPIER, C.A. & SOARES, J.W. (1992): Depósitos de chromita da região do Rio Vila Nova, estado do Amapá. In 37th Congresso Brasileiro de Geologia (São Paulo), 246-247 (abstr.).
- MCCALLUM, M.E., LOUCKS, R.R., CARLSTON, R.R., COOLEY, E.F. & DOERGE, T.A. (1976): Platinum metals associated with hydrothermal copper ores of the New Rambler mine, Medicine Bow Mountains, Wyoming. *Econ. Geol.* **71**, 1429-1450.
- MORENO, T., PRICHARD, H.M., LUNAR, R., MONTERRUBIO, S. & FISHER, P. (1999): Formation of a secondary PGM assemblage in chromitites from the Herbeira ultramafic massif in Cabo Ortegal, NW Spain. *Eur. J. Mineral.* **11**, 363-378.
- MOUNTAIN, B.W. & WOOD, S.A. (1987): Solubility and transport of the platinum-group elements in hydrothermal solutions: thermodynamic and physical chemical constraints. In *Geo-Platinum 87 Symp. Vol.* (H.M. Prichard, P.J. Potts, J.F.W. Bowles & S.J. Cribb, eds.). Elsevier, London, U.K. (57-82).
- _____, _____ (1988): Chemical controls on the solubility, transport and deposition of platinum and palladium in hydrothermal solutions: a thermodynamic approach. *Econ. Geol.* **83**, 492-510.
- NALDRETT, A.J. & DUKE, J.M. (1980): Platinum metals in magmatic sulfide ores. *Science* **208**, 1417-1424.
- NÄSLUND, H.R. & MCBIRNEY, A.R. (1996): Mechanisms of formation of igneous layering. In *Layered Intrusions* (R.G. Cawthorn, ed.). Elsevier, Amsterdam, The Netherlands (1-43).
- NEARY, C.R. & BROWN, M.A. (1979): Chromites from Al 'Ays complex, Saudi Arabia and the Semail complex, Oman. In *Evolution and Mineralisation of the Arabian Nubian Shield* (A.M.S. Al-Shanti, ed.). *Inst. Appl. Geol., Bull.* **2**, 193-205.
- PRICHARD, H.M., IXER, R.A., LORD, R.A., MAYNARD, J. & WILLIAMS, N. (1994): Assemblages of platinum-group minerals and sulphides in silicate lithologies and chromite-rich rocks within the Shetland ophiolite. *Can. Mineral.* **32**, 271-294.
- _____, _____ & LORD, R.A. (1994): Evidence for the mobility of PGE in the secondary environment in the Shetland ophiolite complex. *Trans. Inst. Mining Metall., Sect. B* **103**, 79-86.
- ROBERTS, S. & NEARY, C.R. (1993): Petrogenesis of ophiolitic chromitite. In *Magmatic Processes and Plate Tectonics* (H.M. Prichard, T. Alabaster, N.B.W. Harris & C.R. Neary, eds.). *Geol. Soc., Spec. Publ.* **76**, 257-272.
- ROEDER, P.L. (1994): Chromite: from the fiery rain of chondrules to the Kilauea Iki lava lake. *Can. Mineral.* **32**, 729-746.
- ROWELL, W.F. & EDGAR, A.D. (1986): Platinum-group element mineralisation in hydrothermal Cu-Ni sulphide occurrence, Rathbun Lake, northeastern Ontario. *Econ. Geol.* **81**, 1272-1277.
- STOWE, C.W. (1994): Compositions and tectonic settings of chromite deposits through time. *Econ. Geol.* **89**, 528-546.
- TALKINGTON, R.W., WATKINSON, D.H., WHITTAKER, P.J. & JONES, P.C. (1984): Platinum-group minerals and other solid inclusions in chromite of ophiolitic complexes: occurrence and petrological significance. *Tschermaks Mineral. Petrogr. Mitt.* **32**, 285-301.
- TARKIAN, M. & PRICHARD, H.M. (1987): Irarsite-hollingworthite solid-solution series and other associated Ru-, Os-, Ir-, and Rh-bearing PGMs from the Shetland ophiolite complex. *Mineral. Deposita* **22**, 178-184.
- THALHAMMER, O.A.R. & STUMPFL, E.F. (1988): Platinum-group minerals from Hochgrössen ultramafic massif, Styria: first reported occurrence of PGM in Austria. *Trans. Inst. Mining Metall., Sect. B* **97**, 77-82.

- THAYER, T.P. (1960): Some critical differences between Alpine-type and stratiform peridotite-gabbro complexes. *Int. Geol. Congress, 21st (Norden) XIII*, 247-259.
- TROLY, G., ESTERLE, M., PELLETIER, B.G. & REIBELL, W. (1979): Nickel deposits in New Caledonia, some factors influencing their formation. *In International Laterite Symposium* (D.J.I. Evans, R.S. Shoemaker & H. Veltman, eds.). Soc. Mining Eng. AIME, 85-117.
- ULMER, C.G. (1974): Alteration of chromite during serpentinization in the Pennsylvania – Maryland district. *Am. Mineral.* **59**, 1236-1241.
- VILJOEN, M.J., DE KLERK, W. J., COETZER, P.M., HATCH, N.P., KINLOCH, E. & PEYERL, W. (1986a): The Union section of Rustenburg Platinum Mines Limited, with reference to the Merensky Reef. *In Mineral Deposits of Southern Africa* (C.R. Anhaeusser & S. Maske, eds.). Geological Society of South Africa, Johannesburg, South Africa (1061-1090).
- _____, THERON, J., UNDERWOOD, B., WALTERS, B.M., WEAVER, J.L. & PEYERL, W. (1986b): The Amandelbult section of Rustenburg Platinum Mines Limited, with reference to the Merensky Reef. *In Mineral Deposits of Southern Africa* (C.R. Anhaeusser & S. Maske, eds.). Geological Society of South Africa, Johannesburg, South Africa (1041-1060).
- VOLBORTH, A., TARKIAN, M., STUMPFL, E.U. & HOUSLEY, R.M. (1986): A survey of the Pd–Pt mineralization along the 35-km strike of the J–M reef, Stillwater complex, Montana. *Can. Mineral.* **24**, 329-346.
- VON GRUENEWALDT, G., HATTON, C.J., MERKLE, R.K.W. & GAIN, S.B. (1986): Platinum-group element – chromitite associations in the Bushveld complex. *Econ. Geol.* **81**, 1067-1079.

Received June 10, 1998, revised manuscript accepted January 21, 2001.

APPENDIX: ANALYTICAL TECHNIQUES

Preliminary sampling involved collection of samples from drill core from a widespread coverage of the complex. The subsequent collection focused on detailed and more closely spaced sampling of individual drill cores, including lateritized and non-lateritized material.

Initially, two samples of chromitite from drill core from each of B-1, B-5, C-5 and Samaca chromitite quarry sites (Fig. 1) were analyzed using a Cameca SX-50 electron microprobe at Leeds University. Ten analyses from different grains of chromian spinel within each sample were obtained from each of these eight samples. Typical compositions are given in Table 1, but all the compositions are used in plots. Subsequently, 40 samples of massive chromitite were taken at approximately 75-cm intervals from a unit of chromitite in bore hole GS295 (a drill core from quarry C1), and grains of chromian spinel from these samples were analyzed to determine variation in composition through a layer.

One hundred and thirty-five unlateritized samples of drill core, including chromitite, serpentinite with disseminated chromian spinel (with more than 10% chromian spinel observable in hand specimen), serpentinite with visible sulfides, pyroxenite, and gabbro, were selected for geochemical analysis (Table 2). Each sample was analyzed for Ni, Cu, As and S by atomic absorption, and for Pt and Pd by optical emission spectrography after preconcentration by Te oxide and Sn chloride to remove Fe, at Lakefield Ltd. in Brazil (Table 2). The detection limits were 10 ppb Pt and 2 ppb Pd. The two samples with the highest Pt and Pd values in the chromitites and one sample with the highest Pt and Pd value from both the serpentinite with disseminated chromite and the serpentinite lithological types were selected for analysis by Ni-sulfide fire-assay concentration followed by ICP-MS analysis for all PGE at Genalysis, Western Australia (Table 3). Detection limits of 1–2 ppb are associated with these results. International standard SARM 7 and ETA04 were analyzed at the same time as the samples, and the analyses gave good accuracy and precision. The values obtained for SARM 7 (in ppb) are Ru 430, Rh 225, Pd 1500, Os 58, Ir 78 and Pt 3200, compared with the certified values of Ru 430, Rh 240, Pd 1530, Os 63, Ir 74 and Pt 3740 ppb.

The Pt and Pd values obtained using both methods are similar, as shown by a comparison of pairs of samples PT05 and PT05a, PT18 and PT18a, BC12 and BC12a, and BC104 and BC104a (Tables 2, 3), although the results from Geosol – Minas Gerais are consistently higher, especially for Pd.

During the second phase of sample collection and analysis, six samples of chromitite from GS295 were analyzed for all six PGE at Genalysis, Western Australia, using a Ni sulfide fire-assay concentration and ICP-MS analysis, to examine the variation of PGE with depth in a single layer of chromitite (Table 3). Pt and Pd concentrations in lateritic samples from two adjacent bore holes GS208 and GS209 (drill cores from quarry C5) at a depth of 0.7 to 8.5 meters, together with samples from GS209 at a depth of between 39.6 and 51.10 meters, were analyzed at Genalysis using a Pb collection fire-assay followed by ICP-MS analysis. Trace-element values for all the latter samples were obtained by XRF (Table 4).

Sulfides and PGM (Tables 5 and 6, respectively) were analyzed using a Cambridge Instruments S360 Scanning Electron Microscope interfaced with an Oxford Instruments AN10000 EDX analyzer. Operating conditions for the quantitative analyses were 20 kV, with a specimen calibration current of ~1 nA and a working distance of 25 mm. After every four analyses, the cobalt standard was re-analyzed, in order to check for any drift in the analytical conditions. Images were obtained using a four-quadrant back-scattered electron detector operating at 20 kV, a beam current of ~1 nA, and a working distance of 13 mm, under which conditions magnifications up to 15000 \times are possible. The larger PGM were analyzed quantitatively (Table 6), but those too small for quantitative analysis were analyzed qualitatively. In some cases, PGM were found to be inhomogeneous, and it was only possible to analyze these qualitatively. The presence of Pd and Pt in pentlandite, pyrite and gersdorffite was investigated using a wavelength-dispersion X-ray analysis with a detection limit of 0.05% for Pt and Pd.